Numerical investigation of electrostatically enhanced coalescence of two drops in a flow field

Knut Erik Teigen Giljarhus and Svend Tollak Munkejord
SINTEF Energy Research
P.O. Box 4761 Sluppen
NO-7465 Trondheim, Norway
knut.erik.giljarhus@sintef.no, svend.t.munkejord@sintef.no

Abstract—When an electric field is applied to an emulsion where a conductive fluid is dispersed in an insulating fluid, attractive forces will arise between the drops due to polarization. The drops then tend to coalesce more readily than when no electric field is applied. This phenomenon, often denoted electrocoalescence, is employed for instance to enhance the separation of water from oil extracted from offshore wells. In this work, we employ detailed numerical simulations to study the influence of external flow and electric field on the head-on collision between two drops.

The incompressible Navier-Stokes equations are solved in both the oil and water phase using the finite-difference method. The droplet interface is captured using the level-set method. This allows for incorporating interfacial forces due to interfacial tension and electric field in a consistent manner. The discontinuities in physical properties and other quantities across the interface are handled using the ghost-fluid method. In this method, the discretization stencils are modified near the interface to take into account the physical jump conditions.

To enlighten the physical processes occurring in a separation vessel, we simulate two drops approaching each other in an externally imposed flow field. The influence of fluid properties and the electric field on the coalescence time is investigated.

I. Introduction

When an electric field is applied to an emulsion where a conductive fluid is dispersed in an insulating fluid, attractive forces will arise between the drops due to polarization. The drops then tend to coalesce more readily than when no electric field is applied [1;2]. This phenomenon, often denoted electrocoalescence, is employed for instance to enhance the separation of water from oil extracted from offshore wells. The electrocoalescence process is also of importance to microfluidic devices [3].

A drop collision can be divided into three parts,

1. Drop approach
2. Film drainage
3. Film rupture and coalescence

In the first stage, the drops are brought into contact, typically by an external flow. This external flow determines the collision frequency, the collision force and the collision duration. In the second stage, the thin liquid film between the drops is drained. If the time required to drain the film is shorter than the collision duration, the process continues to the third and final stage where the drops coalesce due to film rupture.

Since water drops in oil typically are small (between 1 and 100μm), we can assume that the collision force is given by a Stokes expression,

$$F \sim 6\pi\mu\dot{\gamma}R^2, \tag{1}$$

where μ is the dynamic viscosity of the oil, $\dot{\gamma}$ is the shear rate and R is the drop radius. The shear rate typically also governs the duration of the collision through the characteristic time $1/\dot{\gamma}$. Film rupture occurs when the film becomes sufficiently thin such that attractive molecular forces become dominant. A simplified expression for the critical film thickness was developed in [4],

$$h_c = \left(\frac{AR}{8\pi\sigma}\right)^{\frac{1}{3}}. \tag{2}$$

Here, σ is the interfacial tension between water and oil, and A is the Hamaker constant, which depends on the fluids.

In this paper, we will investigate the film drainage process. An important non-dimensional number is the capillary number,

$$\mathrm{Ca} = \frac{\mu\dot{\gamma}R}{\sigma}, \tag{3}$$

which relates viscous forces to capillary forces. For low capillary numbers, the interfacial tension is high compared to the viscous forces, which means that the drops will remain relatively undeformed during the drainage process. For high capillary numbers, the front of the drops will become flattened, which means that the drainage process will take longer time [5].

The presence of an electric field can significantly alter this process for a water-in-oil system. Since the oil is insulating and

the water drops are conducting, an attractive force will arise between the drops. A simplified expression for this force is

$$F = \frac{24\pi\varepsilon E_\infty^2 R^6}{h^4}, \tag{4}$$

where h is the distance between the drop centers and E_∞ is the strength of the imposed electric field. We see that the force will rapidly increase as the drops get closer. However, here it is assumed that the drops remain spherical. Instead, they will stretch in the electric field and the tips can become pointed. This will create a sort of wedge which can significantly reduce the drainage time. It is perhaps reasonable to expect that this makes the effect of an electric field higher for higher capillary numbers, since the liquid film radius is larger for higher capillary numbers. However, as we will see later, for realistic electric field strengths, the flattening effect of the external flow dominates over the stretching effect of the electric field. The strength of the imposed electric field, E_∞, is expressed non-dimensionally by the electric capillary number

$$\mathrm{Ca_E} = \frac{\varepsilon R E_\infty^2}{\sigma}, \tag{5}$$

where ε is permittivity of the medium surrounding the drop.

In order to investigate the influence of an electric field on the drainage time, we employ detailed numerical simulations. As a starting point, we look at head-on collisions in a linear, external velocity field. This allows us to simplify the geometry to an axisymmetric configuration, which reduces the computational time significantly compared to full 3D simulations.

II. Mathematical Model and Numerical Methods

The model and numerical method is described elsewhere [6], and will only be briefly revisited here.

We use the level-set method [7] to capture the interface, and solve the full Navier-Stokes equations in each phase. The ghost-fluid method [8] is used to handle the jump conditions on the interface in a sharp manner.

To simulate a conducting liquid in an insulating liquid, it is sufficient to model both liquids as dielectric fluids and set $\varepsilon_{\text{water}} \gg \varepsilon_{\text{oil}}$. In this work, we use $\varepsilon_{\text{water}}/\varepsilon_{\text{oil}} = 250$. To compute the electric forces, we first solve an equation for the electric potential,

$$\begin{aligned} \boldsymbol{\nabla}\cdot(\varepsilon\boldsymbol{\nabla}\psi) &= 0, \\ [\psi] &= 0, \\ [\varepsilon\boldsymbol{\nabla}\psi] &= 0. \end{aligned} \tag{6}$$

Here, the brackets denote jump conditions across the interface. The potential and its gradient are continuous across the interface, but the permittivity is discontinuous. The electric field is then found from

$$\boldsymbol{E} = \boldsymbol{\nabla}\psi. \tag{7}$$

The force is expressed as the divergence of the Maxwell stress tensor,

$$\boldsymbol{F} = \boldsymbol{\nabla}\cdot\mathbf{M}, \tag{8}$$

where the Maxwell stress tensor is given by

$$\mathbf{M} = \boldsymbol{\varepsilon}\left\{\mathbf{E}\otimes\mathbf{E} - \frac{1}{2}(\mathbf{E}\cdot\mathbf{E})\mathbf{I}\right\}. \tag{9}$$

Here, $\mathbf{I}$ is the identity tensor.

The resulting equations are solved in an axisymmetric geometry using the finite-difference method on a stretched, rectilinear grid where the grid spacing is set according to a geometric series. Due to symmetry, only one drop needs to be simulated. An issue with the level-set method is that the drops will automatically coalesce when they are within one grid cell of each other. This means that in order to fully simulate the film drainage process, the first grid point should be at the critical film thickness, which can be approximated by Eq. (3). This is unfortunately not possible due to high computational cost. Nonetheless, we believe that the results still provide valuable insights.

III. Results

The computational setup is illustrated in Fig. 1. We use a computational domain of size $4R \times 4R$, and a grid size of 80×80. To get higher resolution in the coalescence region, the grid spacing is varied according to a geometric series with a stretching factor of 1.025. An initial velocity field is imposed according to

$$\boldsymbol{U}(r,z) = \frac{\dot{\gamma}}{2}(-r, 2z). \tag{10}$$

The viscosity ratio is set to $\mu_{\text{water}}/\mu_{\text{oil}} = 0.01$. An example of the initial velocity field and electric field is shown in Fig. 2. Herein, the symmetry planes have been "unwrapped" for illustration purposes.

In [5], the coalescence time is defined as the time from when the drop centers are $2R$ apart, to the time of coalescence. With an electric field, the drops may coalesce before the distance is $2R$ due to the formation of pointed tips. We therefore use the full time from the initial state to the coalescence as the coalescence time here.

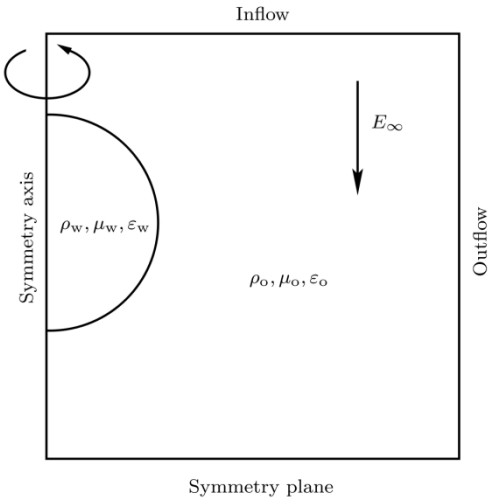

Figure 1. Illustration of computational setup.

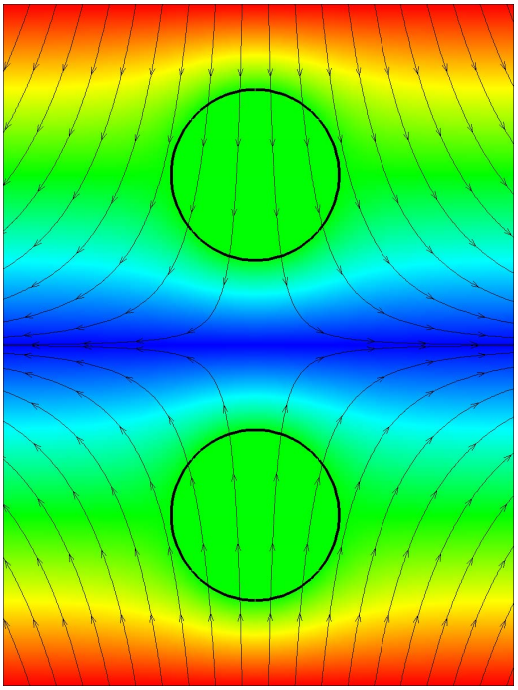

Figure 2. Example of initial configuration. The streamlines indicate the imposed velocity field, the colour shows the electric potential and the circles denote the drop interface.

We performed simulations at capillary numbers ranging between 10^{-3} and 10^{-1}, and electric capillary numbers ranging between 10^{-3} and 10^{-2}. The resulting drop shapes when no electric field is applied are shown in Fig. 3. As the capillary number increases, the drop deforms more and more, and the intervening film becomes bigger. This also means it will take a longer time to drain the film, and the coalescence time is longer. This trend is evident from Fig. 4 which shows the coalescence time as a function of capillary number.

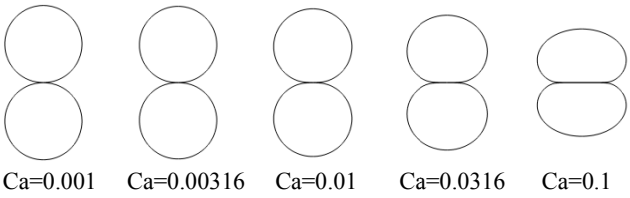

Figure 3. Drop shapes at coalescence for capillary numbers varying logaritmically between 10^{-3} and 10^{-1}.

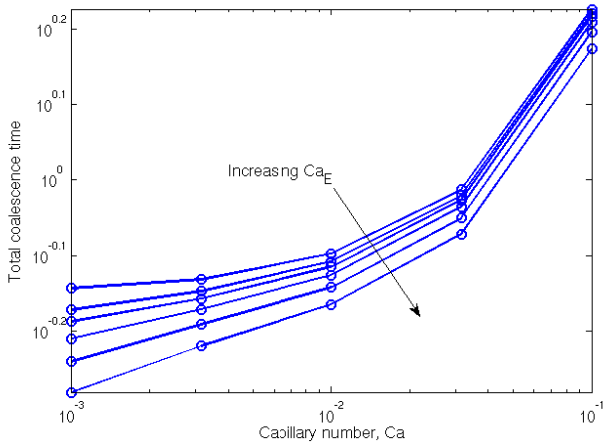

Figure 4. The coalescence time as a function of capillary number for electric capillary numbers varying logaritmically between 10^{-3} and 10^{-2}.

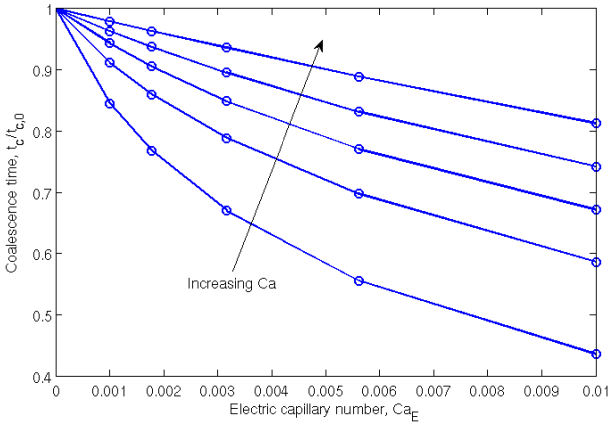

Figure 5. The coalescence time scaled by the coalescence time with no electric field, plotted as a function of electric capillary number for capillary numbers varying logarithmically between 10^{-3} and 10^{-1}.

The graph in Fig. 4 also shows the results at varying electric capillary numbers. Since the electric capillary numbers here are relatively low (which is representative for an industrial application), the actual drop shapes are not influenced much by the electric field. However, the coalescence time is still significantly reduced. By plotting the coalescence time as a function of the electric capillary number, the influence of the electric field can be shown more clearly. This is done in Fig. 5. Here, we see that for low capillary numbers, the coalescence time can be cut by more than 50% by utilizing an electric field. When the capillary number is increased, this effect is reduced, and for high capillary numbers, the coalescence time is only reduced by 20%, even for high electric field strengths. This information can be directly applied to an industrial context. In an industrial electrocoalescer, some degree of turbulence is usually present. This is advantageous, since it increases the amount of collisions, which in turn increases the sedimentation rate. But the turbulence can also tear drops apart, which reduces the efficiency. Here, we also see that too high turbulence can reduce the coalescence efficiency of the collisions. This is already known from e.g. [5]. What is new is

that high capillary numbers also appear to significantly reduce the effect of an electric field.

IV. Conclusions

The effect of an electric field on the head-on collision between two drops in an external flow was investigated numerically. A detailed model solved using a high-resolution numerical method was employed. It was shown that the coalescence time increases with increasing capillary number. Next, it was demonstrated that the presence of an electric field reduces the coalescence time. For low capillary numbers, the reduction was more than 50% for high field strengths. For higher capillary numbers, however, the effect of an electric field was reduced.

Acknowledgement

This work is funded by the project “Electrocoalescence – Criteria for an efficient process in real crude oil systems” co-ordinated by SINTEF Energy Research. The project is supported by The Research Council of Norway, under the contract no: 169466/S30, and by the following industrial partners: Aker Solutions AS, BP Exploration Operating Company Ltd, Hamworthy Technology and Products AS, Shell Technology Norway AS, Petrobras, Saudi Aramco and Statoil ASA.

Bibliography

[1] P. Atten, "Electrocoalescence of Water Droplets in An Insulating Liquid," *Journal of Electrostatics*, vol. 30, pp. 259-269, May1993.

[2] J. S. Eow, M. Ghadiri, A. O. Sharif, and T. J. Williams, "Electrostatic enhancement of coalescence of water droplets in oil: a review of the current understanding," *Chemical Engineering Journal*, vol. 84, no. 3, pp. 173-192, Dec. 2001.

[3] K. Ahn, J. Agresti, H. Chong, M. Marquez, and D. A. Weitz, "Electrocoalescence of drops synchronized by size-dependent flow in microfluidic channels," *Applied Physics Letters*, vol. 88, no. 26 June2006.

[4] A.K. Chesters, "The modelling of coalescence processes in fluid-liquid dispersions : a review of current understanding," *Chemical engineering research & design*, no. A4, pp. 259-270, 1991.

[5] L.G. Leal, "Flow induced coalescence of drops in a viscous fluid," *Physics of Fluids*, vol. 16, no. 6, pp. 1833-1851, 2004.

[6] K. E. Teigen and S. T. Munkejord, "Sharp-interface Simulations of Drop Deformation in Electric Fields," *IEEE Transactions on Dielectrics and Electrical Insulation*, vol. 16, no. 2, pp. 475-482, Apr.2009.

[7] S. Osher and R. P. Fedkiw, "Level set methods: An overview and some recent results," *Journal of Computational Physics*, vol. 169, no. 2, pp. 463-502, May2001.

[8] R. P. Fedkiw, T. Aslam, B. Merriman, and S. Osher, "A non-oscillatory Eulerian approach to interfaces in multimaterial flows (the ghost fluid method)," *Journal of Computational Physics*, vol. 152, no. 2, pp. 457-492, July1999.